Supporting Online Material

Materials and Methods:

Proteins, Reagents, and ATPase Assays: All experiments were performed in KMg25 (10 mM Mops, pH 7.0, 25 mM KCl, 1 mM MgC_2, 1 mM EGTA, 5 mM dithiothreitol) at ~23 °C. Actin was purified from rabbit skeletal muscle as described (*1*) and stabilized with rhodamine-phalloidin. A truncated myo1b isoform-b (residues 1-831) construct containing a C-terminal 15-amino acid sequence for site-specific biotinylation (AviTag) was expressed, purified, and biotinylated as described (*2*). N-ethylmaleimide (NEM) modified skeletal muscle myosin-II was prepared as described (*2, 3*). All chemicals and reagents were from Sigma (St. Louis, MO), unless specified otherwise.

Steady-state ATPase activities were measured in KMg25 using the NADH-coupled assay as described (*4*). Transient phosphate release was measured by a sequential mix stopped-flow method using the coupled assay system containing the fluorescently labeled mutant of the phosphate binding protein as described (*5*).

Polystyrene beads (1.1 μm, Sigma) were washed twice with water and incubated with NEM-myosin-II (~2 mg/ml in 500 mM KCl, 4 mM $MgCl_2$, 1 mM EGTA, 20 mM K phosphate buffer, pH 7.2) for 1 hr at 4 °C. NEM-Myosin-II coated-beads were collected by centrifugation in the presence of 1 mg/ml BSA and resuspended in KMg25.

Motility Chamber Preparation: Nitrocellulose-coated motility chambers containing 1.9 μm silica beads as pedestals (Bangs Laboratories, Fishers, IN) were prepared as described (*6*). Solutions were added sequentially to the chamber as follows: 0.1 mg/ml streptavidin in water (3 min), 1 mg/ml bovine serum albumin in KMg25 (2 x 5 min), 1 – 5 nM biotinylated myo1b in

KMg25 + 10 µM calmodulin (5 min), 1 nM rhodamine-phalloidin labeled F-actin in KMg25 with 10 mg/ml glucose, 1 - 50 µM ATP, 10 µM calmodulin, 192 U/ml glucose oxidase, and 48 µg/ml catalase (Roche). Beads coated with NEM-myosin-II were added to one side of the chamber to replace ~¼ the volume of the chamber. The chamber was sealed with silicon vacuum grease (Dow Corning, Midland, MI).

Single Molecule Force and Displacement Measurements: Optical trap experiments were performed using a dual-trap instrument as described (*6*). Trap stiffnesses were ~0.022 pN / nm. NEM-myosin-II beads were captured in separate optical traps, and bead-actin-bead dumbbells were assembled by contacting trapped beads with individual actin filaments. Bead-actin-bead assemblies were pretensioned to ~2 pN and lowered onto the surface of a pedestal using a piezoelectric stage to scan for actomyo1b interactions. Upon observation of interactions, data were digitized with a 2 kHz sampling rate for 6 - 10 minute intervals. Motility chambers were used for < 90 min after preparation.

The force-dependence of actomyo1b attachment lifetimes was measured using a feedback system that applies a dynamic load to the actomyo1b to keep the actin near its isometric position during the myosin working stroke as described (*6*). Briefly, changes in the force on the bead attached to the pointed end of the actin filament (transducer bead) were fed through an analog integrating feedback amplifier to an acousto-optic deflector, which changed the position of the laser trap on the bead bound to the barbed end of the actin filament (motor trap) until the position of the transducer bead was restored to its original position. The response time of the feedback loop in the absence of interactions was adjusted to 50 ms for each bead-actin-bead assembly.

Event Selection and Ensemble Averaging: Events were selected using the covariance threshold method described in (*6*) using in-house software written in Labview. The variance of the digitized forces on the transducer and motor beads was calculated at each time point of the data files over an 85 ms sliding-window and the resulting signal was smoothed over a 50 ms sliding-window. The covariance was then calculated as described (6). A typical set of force and covariance traces and a histogram of the covariance data from the top trace in Fig. 1A are shown in Fig S1.

Two methods were used to determine the start and ends of actomyo1b attachments. Selection method #1 was used to minimize false positives in the attachment-duration measurements (Figs 2A & S2). Attachment starts were defined as the point when the covariance decreased from the peak of the distribution of covariances assigned to actin detached from myo1b (point A in Fig. S1) and reached the peak of the covariance distribution assigned to actin bound to myo1b (point B in Fig. S1). Attachment ends were defined as the point when the covariance returned to the peak of the detached covariance distribution.

Selection method #2 was used to optimize the time resolution of the time courses of the ensemble averages presented in Figs. 1B & 3A. Attachment starts were defined as the point when the covariance decreased below a point between the attached and detached covariances where the histogram of covariances was a minimum (point C in Fig. S1). Attachment ends were defined as the point where the covariance went above that same threshold (point C in Fig. S1). Since these selection criteria resulted in a greater number of false positive events, the total ensemble averaged events were normalized by the number of events identified by selection method #1.

Ensemble averages of interactions that were synchronized at the times the interactions started or ended were performed as described (*7*). Briefly, events were synchronized to the start or end of each event as determined by selection method #2 (above), and events were extended (forwards or backwards in time, respectively) based on the force value at the covariance threshold for each event. Time courses of the ensemble averages were fit to single exponential rate functions (k_{obs} = Amplitude(1 - $e^{-rate \times time}$) using Kaleidagraph. Best fit parameters and standard errors of the fits are reported. For feedback event sorting, ensemble averages of event starts and ends were binned by the force immediately prior to detachment.

Maximum Likelihood Estimation

Bootstrap Monte Carlo simulations were performed to generate data for Maximum Likelihood Estimations (MLEs) of the log-likelihood of eq. 2 (*8, 9*) in Mathcad (Mathsoft). A range of all applicable parameters was tested to find the peak in the log likelihood, and the parameters corresponding to this peak were reported as the best-fit values. Errors were assessed at a 97% confidence level. The calculated MLEs from the simulated data were normalized according to the MLE from the original data set. If the value was less than 2-standard deviations away, it was rejected. The parameters from the accepted set were collected and the maximum and minimum values were recorded. Errors were obtained by subtracting the maximum and minimum values from the respective parameters.

References:

1. J. A. Spudich, S. Watt, *J Biol Chem* **246**, 4866 (Aug 10, 1971).
2. T. Lin, N. Tang, E. M. Ostap, *J Biol Chem* **280**, 41562 (Dec 16, 2005).
3. C. Veigel, M. L. Bartoo, D. C. White, J. C. Sparrow, J. E. Molloy, *Biophys J* **75**, 1424 (Sep, 1998).
4. E. M. De La Cruz, H. L. Sweeney, E. M. Ostap, *Biophys J* **79**, 1524 (Sep, 2000).
5. J. H. Lewis, T. Lin, D. E. Hokanson, E. M. Ostap, *Biochemistry* **45**, 11589 (Sep 26, 2006).
6. Y. Takagi, E. E. Homsher, Y. E. Goldman, H. Shuman, *Biophys J* **90**, 1295 (Feb 15, 2006).
7. C. Veigel, J. E. Molloy, S. Schmitz, J. Kendrick-Jones, *Nat Cell Biol* **5**, 980 (Nov, 2003).
8. W. H. Press, S. A. Teukolsky, W. T. Vetterling, B. P. Flannery, *Numerical Revipes in C++*. (Cambridge University Press, New York, 2002).
9. P. R. Bevington, Robinson, D. K., *Data Reduction and Error Analysis for the Physical Sciences*. (McGraw-Hill, New York, 2003).

Supplementary Figure Legends

Supplementary Figure 1. Selection of actomyo1b interactions. (A) Forces on the two trapped beads holding a single actin filament during an actomyo1b interaction. (B) Covariances of the trapped beads calculated for the trace shown above. Points A, B, and C correspond to the covariances identified on the histogram below. (C) Distribution of the covariances from the top trace in Fig 1A, which includes the interaction shown above. The histogram is bimodal with the higher covariance distribution corresponding to the detached state and the lower distribution corresponding to the actomyo1b attached state. The cutoff thresholds for the two types of analyses are shown as colored bars. When selecting events for analysis of attachment durations, the green threshold (mean covariance of the attached state, point B) determines the beginning of the event, while the red threshold (mean covariance of the detached state, point A) determines the end of the event. When selecting events for ensemble averaging, the black covariance threshold (point C) is used to determine the start and end point of events.

Supplementary Figure 2. (A) Frequency distributions of actomyo1b attachment durations at low trap stiffness (0.022 pN/nm) at different ATP concentrations. Solid lines show distributions that were calculated according to the two-step model shown in the lower-right panel. The values of k_{start} and k_{end} used in the calculation were obtained from the start- and end-time ensemble averages presented in Figure 1.

Supplementary Figure 3. Steady-state ATPase activity and transient phosphate release from actomyo1b. (●) The actin dependence of the steady-state ATPase rate of myo1b measured using

the NADH-coupled assay at 23 °C. (○) Actin dependence of the rate of phosphate release from 2.5 μM myo1b in the presence of 0 – 100 μM actin, 1.25 μM ATP, and 5.0 μM phosphate binding protein. High viscosity of the samples limited our ability to acquire data at > 100 μM actin. The solid line is a fit of the steady-state ATPase rates to the Michaelis-Menten equation, yielding V_{max} = 0.38 ± 0.14 $s^{-1}$and K_M = 310 ± 160 μM. The maximum steady-state ATPase rate (V_{max}) is limited by the rate of phosphate release and can be taken as the phosphate release rate for myo1b (*5*).

Supplementary Figure 4. Time courses of ensemble averages of (left) starts and (right) ends of actomyo1b interactions acquired with the isometric clamp in the presence of 50 μM ATP. Interactions were sorted into bins based on the force immediately before detachment. In the end-time averages, forces decreased before the substep transient that precede detachment. Additionally, the averages of starts have higher forces than the averages of ends because detachment preferentially occurs during the low point of the fluctuations of force (i.e., noise) on the actomyo1b. The decreases in force prevent the direct determination of k_{start} from the force-binned ensemble averages.

Supplementary Figure 5. Model for the molecular function of myosin-I. Myosin-I, attached to a specific cargo or membranes, interacts with actin and generates a displacement that stretches a cellular "spring." This spring may be the deformation of membranes during endocytosis, the deformation of stiff actin networks during the transport of membranes or vesicles, or the tensioning of mechano-sensitive ion channels in the adaptation response of sensory hair cells. Tension on myosin-I results in a dramatically reduced rate of ADP release, and the myosin acts

as an anchoring-protein with an attachment lifetimes > 45 s. When strain on the spring is reduced via membrane or protein movements, ADP is released, and active ATP cycling and motility of the motor complex resume.

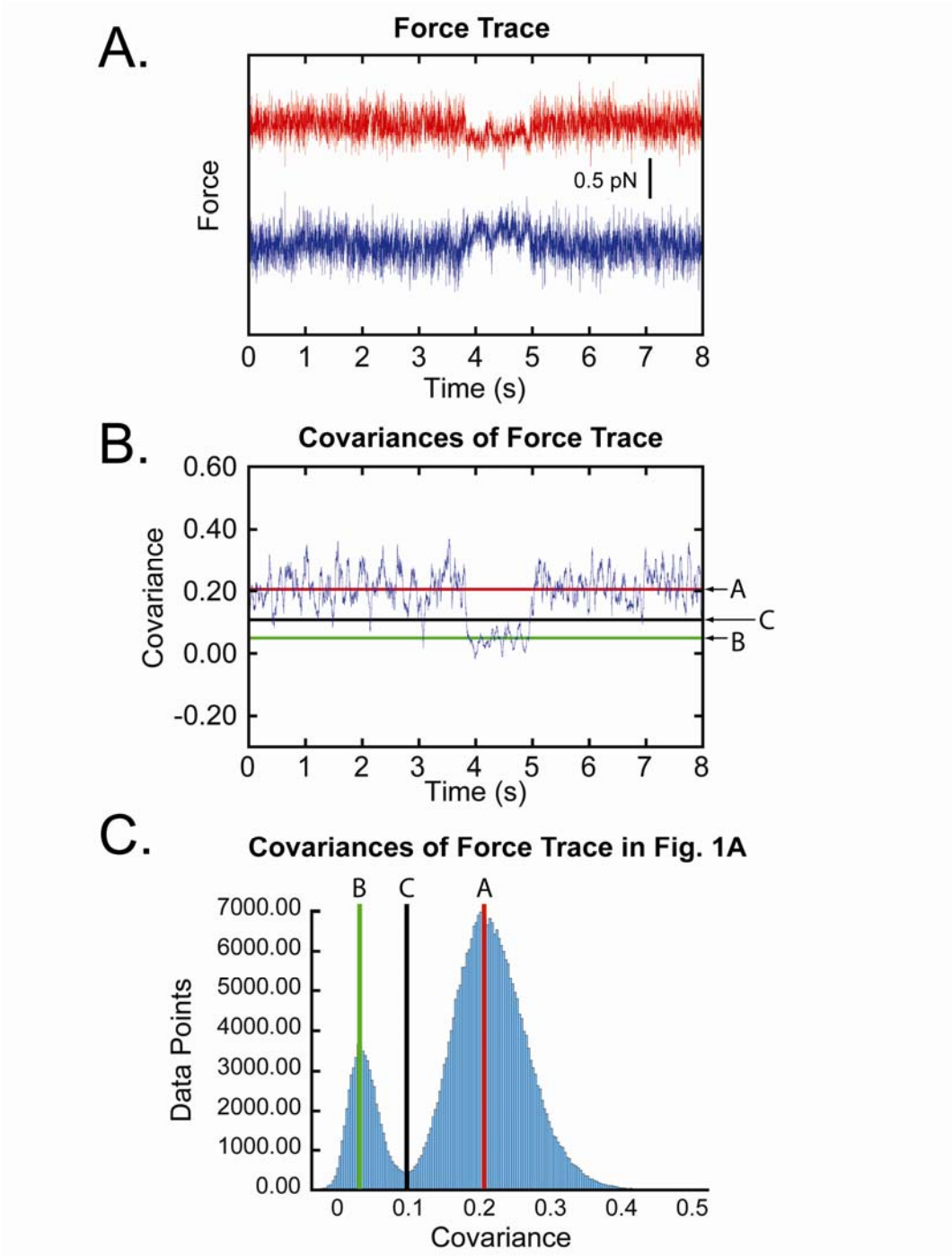
A.
Force Trace
Force
0.5 pN
0 1 2 3 4 5 6 7 8
Time (s)
B.
Covariances of Force Trace
Covariance
0.60
0.40
0.20
0.00
-0.20
A
C
B
0 1 2 3 4 5 6 7 8
Time (s)
C.
Covariances of Force Trace in Fig. 1A
B
C
A
Data Points
7000.00
6000.00
5000.00
4000.00
3000.00
2000.00
1000.00
0.00
0 0.1 0.2 0.3 0.4 0.5
Covariance

Figure S1.

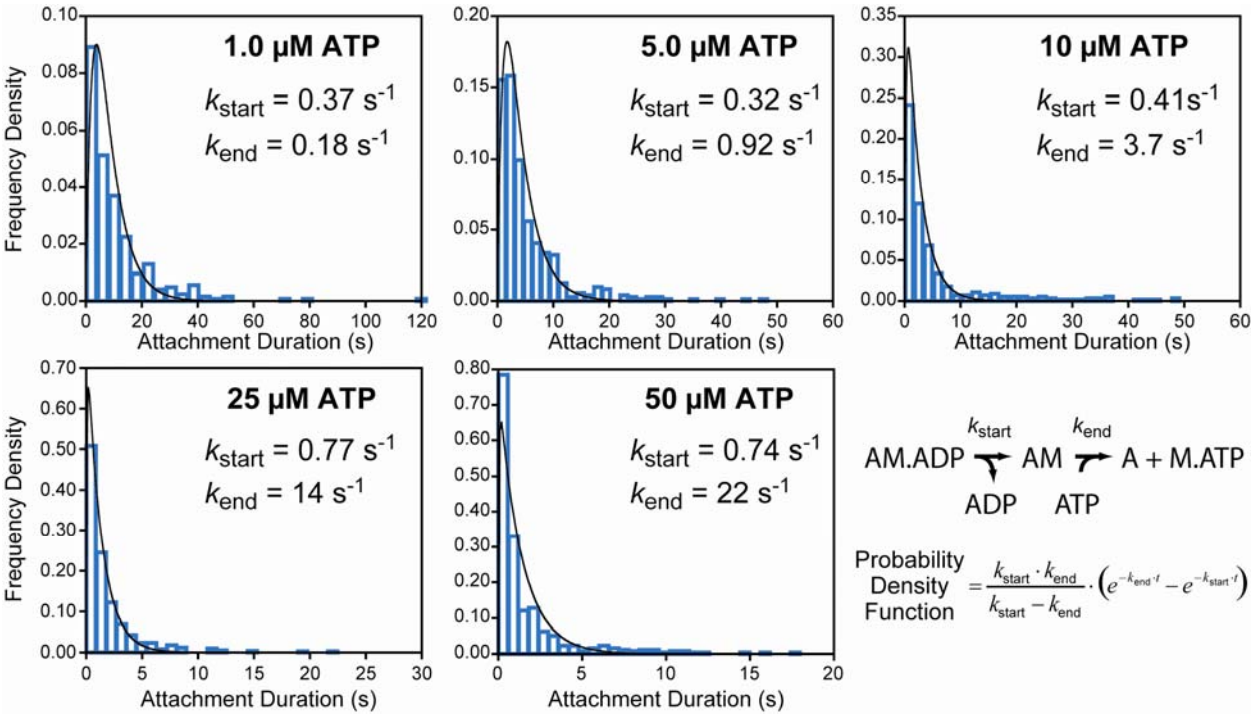
1.0 μM ATP
k_{start} = 0.37 s^{-1}
k_{end} = 0.18 s^{-1}
5.0 μM ATP
k_{start} = 0.32 s^{-1}
k_{end} = 0.92 s^{-1}
10 μM ATP
k_{start} = 0.41s^{-1}
k_{end} = 3.7 s^{-1}
25 μM ATP
k_{start} = 0.77 s^{-1}
k_{end} = 14 s^{-1}
50 μM ATP
k_{start} = 0.74 s^{-1}
k_{end} = 22 s^{-1}
Frequency Density
Attachment Duration (s)
AM.ADP ⇌ AM → A + M.ATP
ADP
ATP
Probability Density Function $= \frac{k_{start} \cdot k_{end}}{k_{start} - k_{end}} \cdot \left(e^{-k_{end} \cdot t} - e^{-k_{start} \cdot t}\right)$

Figure S2.

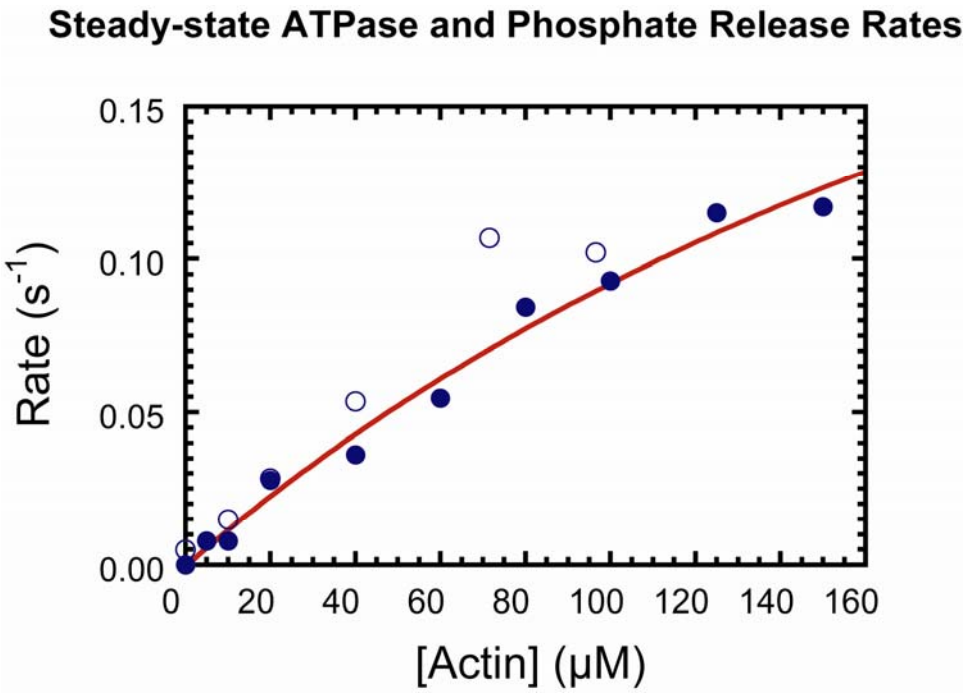
Steady-state ATPase and Phosphate Release Rates
Rate (s^{-1})
0.15
0.10
0.05
0.00
0
20
40
60
80
100
120
140
160
[Actin] (μM)

Figure S3.

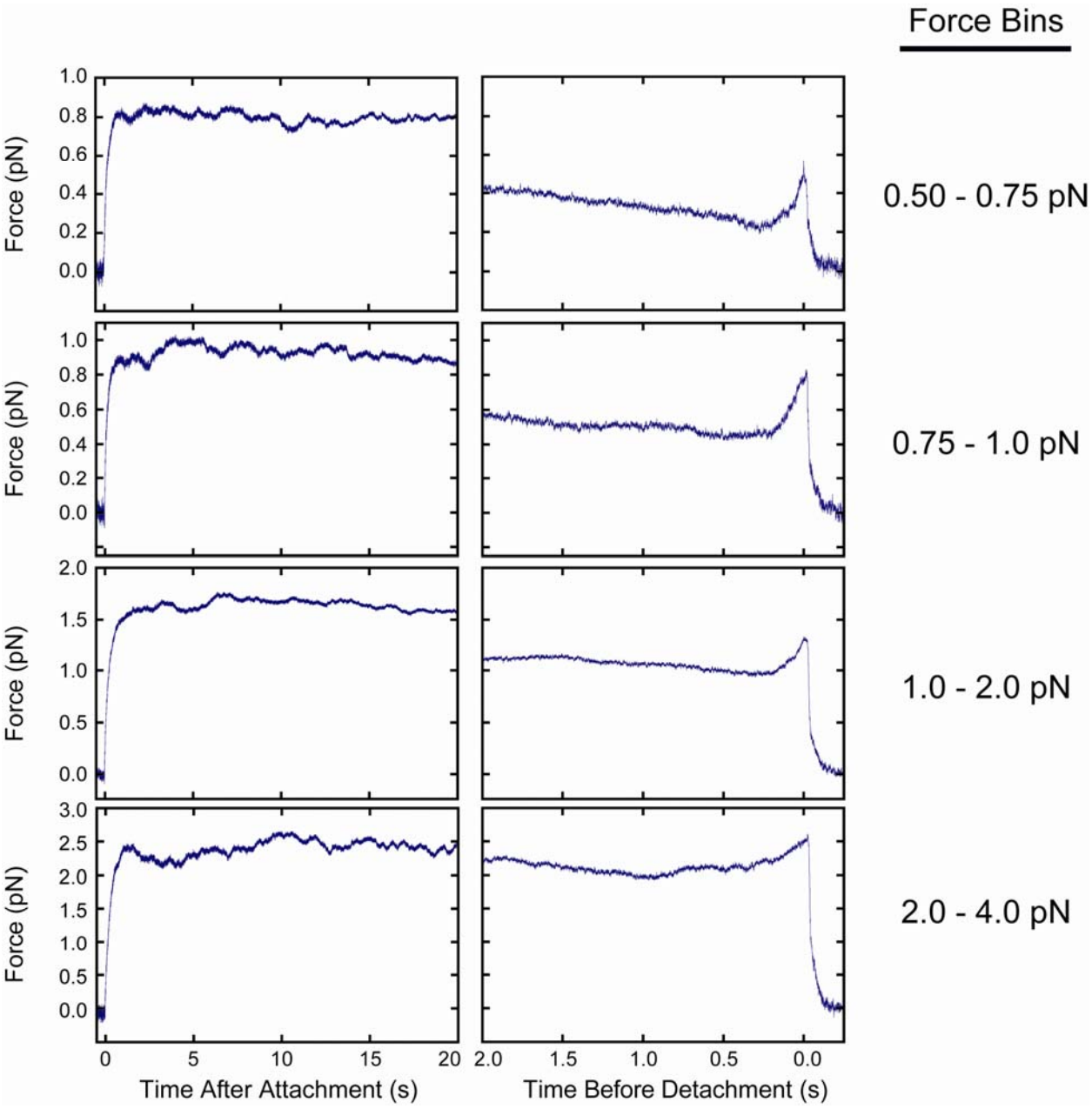
Force Bins
0.50 - 0.75 pN
0.75 - 1.0 pN
1.0 - 2.0 pN
2.0 - 4.0 pN
Force (pN)
Time After Attachment (s)
Time Before Detachment (s)

Figure S4.

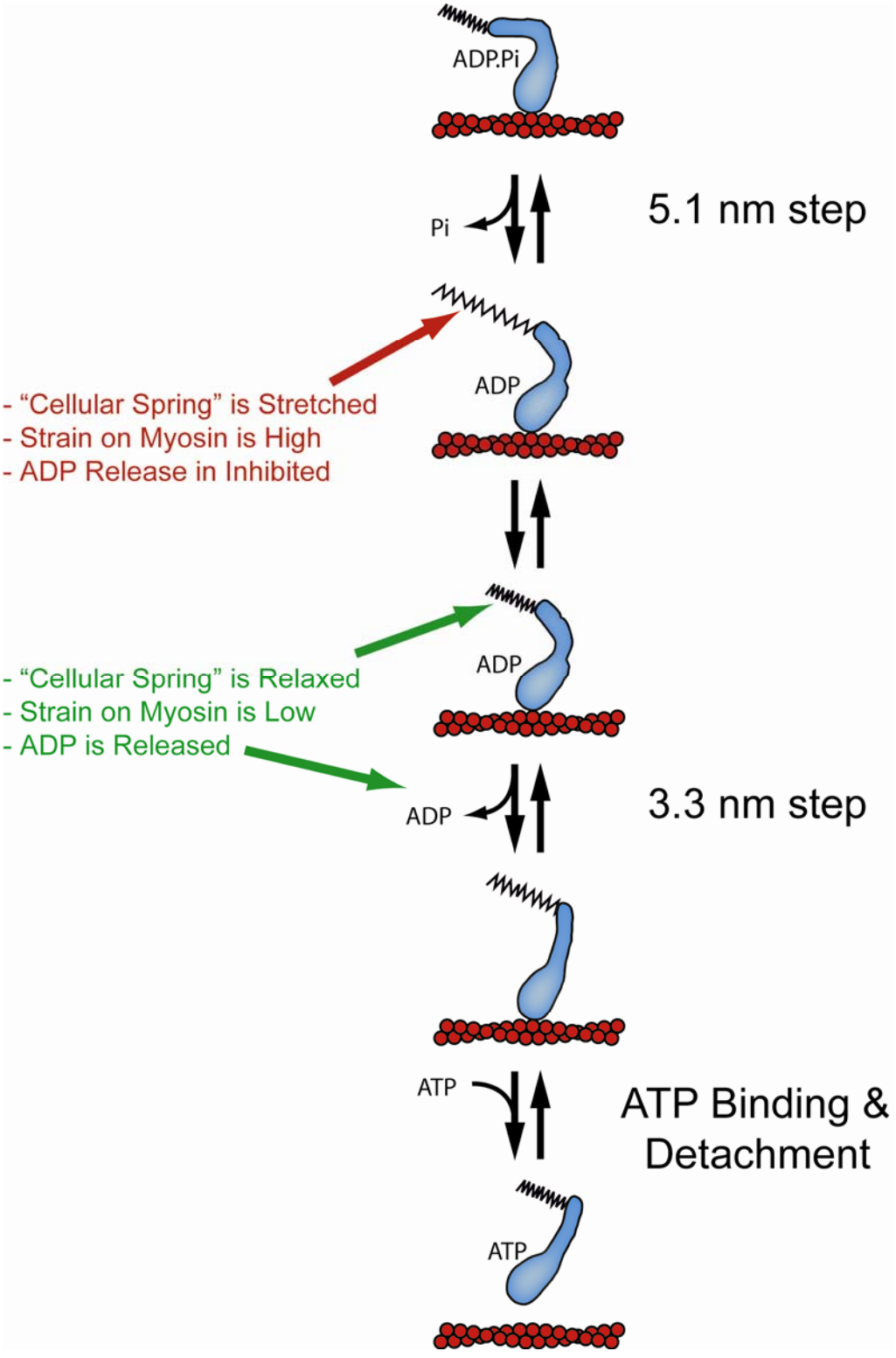
ADP.Pi
Pi
5.1 nm step
ADP
- “Cellular Spring” is Stretched
- Strain on Myosin is High
- ADP Release in Inhibited
ADP
- “Cellular Spring” is Relaxed
- Strain on Myosin is Low
- ADP is Released
ADP
3.3 nm step
ATP
ATP Binding &
Detachment
ATP

Figure S5.